Disk-shaped Compact Tension Test for Plain Concrete

A. Amirkhanian[1], D. Spring[1], J. Roesler[1], K. Park[1], G. Paulino[1]

[1]Dept. of Civil Eng., Univ. of Illinois at Urbana–Champaign, 205 N. Mathews Ave., Urbana, IL 61801

Abstract

The estimation of concrete fracture properties is essential for an accurate cracking prediction of concrete pavement systems. The single-edge notched beam test has been used to characterize fracture parameters of concrete materials in the laboratory, but obtaining a field specimen with this geometry is not always practical. Currently, a standard exists, ASTM D7313, for the measurement of fracture energy in asphalt concrete using the disk-shaped compact tension (DCT) test. The benefit of this specimen geometry for both concrete and asphalt is that it can easily be fabricated in the laboratory or cored from the field. The total fracture energy (G_F) of the material is estimated by using the concept of the work-of-fracture. Additional properties, such as the initial fracture energy (G_f) and the critical crack tip opening displacement ($CTOD_C$), can be extracted from the same test through employing compliance measurements and the concept of an equivalent elastic crack model. In this pilot study, the DCT specimen is adopted for concrete materials with small changes to the hole and notch geometry and loading rate of the specimen relative to ASTM D7313. The initial DCT experimental results for concrete containing virgin limestone aggregate and recycled concrete aggregate have been consistent and repeatable. A finite element model (FEM) of the specimen was developed to check the published K_{IC} equation for this geometry and to derive the $CTOD_C$ correction factor. A cohesive zone model was also successfully implemented to simulate the DCT specimen, which verified the validity of the calculated fracture properties from the DCT experiments.

Introduction

Future improvements to mechanistic-based design methods for concrete pavements will require properties that account for the concrete material's crack growth resistance. Current pavement designs utilize the flexural strength of the concrete and fatigue relationships to completely describe the slab's failure. These empirical models do not adequately predict the service life of concrete pavements without significant calibration of the fatigue damage models (Beckett and Humphreys 1989; Falkner and Teutsch 1993; Roesler 1998; Ioannides 2005; Rao and Roesler 2004; Roesler et al. 2005). Recent progress has been made to quantify the flexural capacity of concrete slabs using fracture properties of the concrete in conjunction with a cohesive crack model in a finite element framework (Ioannides et al. 2006, Gaedicke et al. 2009a, Gaedicke 2009b).

The key inputs to the cohesive crack models are fracture and strength properties. The tensile strength can be estimated by the split tensile test or calculated by optimizing the softening curve to the test data. The most common specimen type to measure concrete fracture quantities has been a notched or unnotched three-point beam test (e.g., Jenq and Shah 1985, RILEM 1990, Guinea et al. 1994, Planas et al. 1999, Bažant et al. 2002a, Bažant 2002b, Cusatis and Schauffert 2009). However, because of its geometry and the

geometry of other specimen types (e.g., wedge split test by Brühwiler and Wittmann 1990), the use of these fracture tests are limited to laboratory cast samples. Recent work on the disk-shaped compact tension (DCT) specimen geometry has shown it to give accurate and reliable load-CMOD curves and fracture energy values for asphalt concrete materials at low temperatures (Wagoner et al. 2005, 2006; Kim, H. and Buttlar 2009, Kim, M. and Buttlar 2009, Zofka and Braham 2009). Some research has been done on compact tension (CT) specimens for concrete (Van Mier 1991; Issa et al. 2000a,b; Kumar and Barai 2009) but no studies were found on a DCT specimen. The main advantage of the DCT over the CT specimen geometry is it can easily be extracted from field concrete slabs with a coring machine, which is the primary motivation of this work.

Research Objective

The objective of this study is to evaluate the viability of DCT geometry, similar to ASTM D7313, for testing two types of concrete material fracture properties. In this initial work, the exact DCT specimen geometry is taken from Tada et al. (2000) because the K_I and CMOD geometric factors are already available. The second objective is to extract concrete fracture properties and to simulate the fracture response of the two concrete materials (i.e. limestone coarse aggregate (LCA) and a recycled concrete aggregate (RCA) concrete) in the DCT specimen configuration using a finite element-based cohesive zone model.

Experimental Procedure

Multiple concrete slabs measuring 2.2m by 2.2m by 15cm thick were cast with either limestone coarse aggregate (LCA) or recycled concrete aggregate (RCA). The mixture proportions for the two types of concrete slabs are shown in Table 1.

Table 1. Concrete mix design for specimens.

Material	Quantity [kg/m^3]
Cement	246
Class C Fly Ash	61
Coarse Aggregate: Limestone or RCA	1019
Fine Aggregate: Natural Sand	774
Water	129
HRWR	As needed

After curing for three months, four cores (144 mm diameter) were taken from each LCA and RCA concrete slab and then cut to match the DCT geometry specified in Figure 1. Two DCT specimens could be fabricated from each 15cm thick core. Additional cores were taken to measure the concrete's compressive and tensile strengths (Table 2). The compressive strength of the LCA concrete higher than the RCA concrete but this trend was not seen in the split tensile test results. The elastic modulus was calculated according to the ACI Building Code (ACI 318) as a standard specimen could not be obtained from the slab specimens.

A servo-hydraulic testing frame was used to apply the load and a clip-on strain gage was mounted to control and measure opening deformations at the edge of the specimen as

shown in Figure 2. The specimens were seated with a 0.2 kN load and then loaded with a crack mouth opening displacement (CMOD) rate of 0.1 mm/min. Once the peak load was reached, the specimen was unloaded at 0.2 kN/sec until the seating load was reached. This loading and unloading was completed to calculate the initial fracture properties of the specimen based on the two-parameter fracture model (Jenq and Shah 1985). The specimen was reloaded at the initial rate until the concrete had softened to 0.2 kN.

Table 2. Concrete strength properties.

Slab Specimen	Compressive Strength [MPa]	Split Tensile Strength [MPa]	Split Tensile Strength COV	Elastic Modulus* [GPa]
Limestone	50.2	3.3	10.3%	33.5
RCA	39.2	3.2	7.7%	29.6

*Calculated from compressive strength

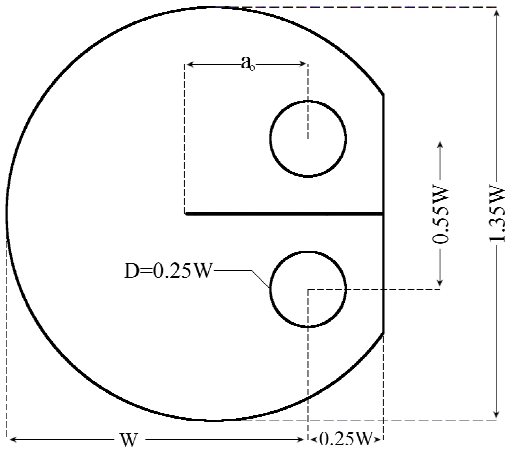

Dimension	Value [mm]
W	106.9
D	26.7
a_o	44.3
Thickness (B)	51.0

Figure 1. DCT specimen dimensions, adapted from Tada et al. (2000).

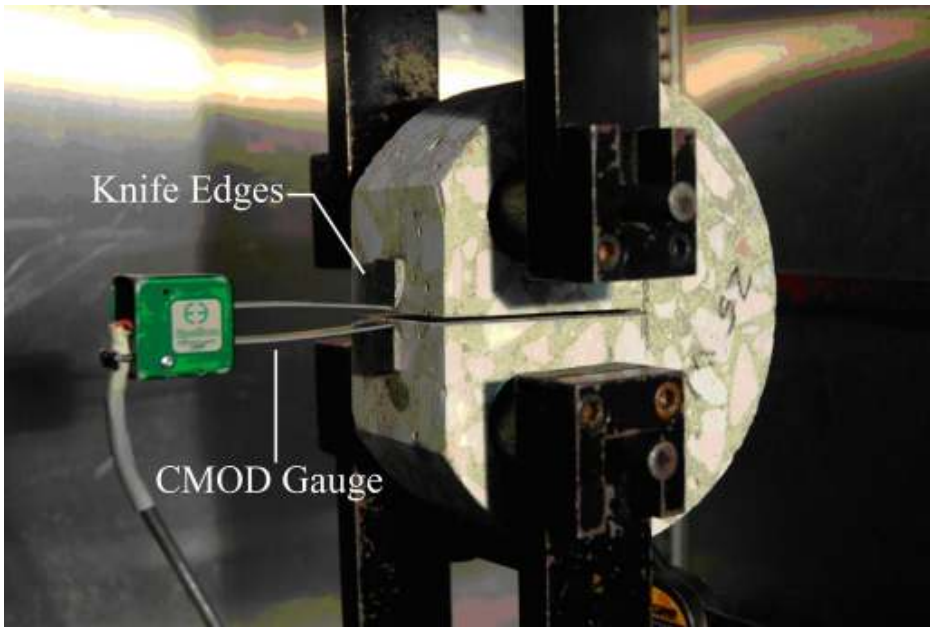

Figure 2. Specimen setup for the DCT test.

The load-CMOD plots for the LCA and RCA specimens are presented in Figures 3 and 4. A summary of the peak loads for the two material types can be found in Table 3 with an average of 1.39 kN (st. dev. = 0.16 kN) and 1.02 kN (st. dev. = 0.06 kN) for the LCA and RCA concrete, respectively. The initial load and CMOD results suggest the DCT specimen was a repeatable test with the average COV less than 15 percent.

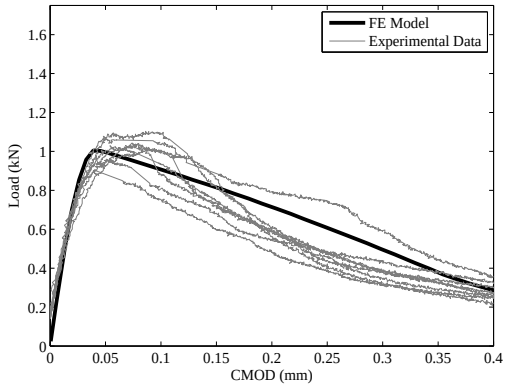

Figure 3. DCT experimental and FE model load versus CMOD results for concrete containing limestone coarse aggregate.

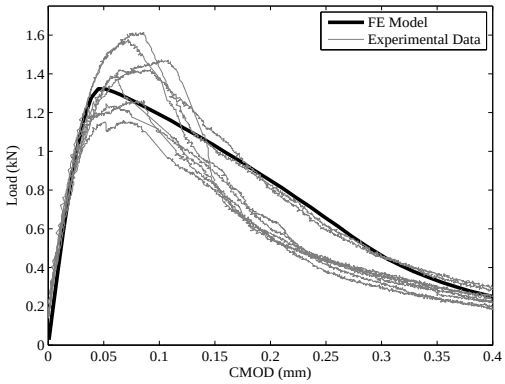

Figure 4. DCT experimental and FE model load versus CMOD results for concrete containing recycled concrete aggregate

Concrete Fracture Properties

The finite element modeling of the DCT configuration requires the concrete's fracture properties, such as the critical stress intensity factor (K_{IC}), critical crack tip opening displacement ($CTOD_C$), and the total fracture energy (G_F). The initial fracture properties (K_{IC} and $CTOD_C$) can be determined from the Two-Parameter Fracture Model (TPFM) by Jenq and Shah (1985). Equations to calculate these quantities are needed to relate the critical crack length at the peak load to the specimen geometry. First, the initial loading concrete stiffness (E_i) can be calculated from equation 1.

$$E_i = \frac{WV_{CMOD}(\alpha_o)}{C_i} \tag{1}$$

The initial compliance, C_i, was taken to be the inverse slope of the initial P-CMOD curve from the seating load to 50 percent of the peak load. The CMOD geometric factor, $V_{CMOD}(\alpha_o)$, for the DCT geometry (Tada et al. 2000) is given in eq. 2. The initial notch depth ratio, $\alpha_o = a_o/W$ is corrected for the knife edge thickness, h, and shown in the general form (eq. 3).

$$V_{CMOD}(\alpha) = \exp\left(1.742 - 0.495\alpha + 14.71\alpha^2 - 22.06\alpha^3 + 14.44\alpha^4\right) \tag{2}$$

$$\alpha = \frac{a+h}{W+h} \tag{3}$$

The unloading compliance, C_u, can also be used to calculate the concrete stiffness (E_u) after the peak load has been reached. The unloading compliance was experimentally

determined as the inverse slope of the unloading P-CMOD curve from 80 percent of the peak load to 20 percent of the peak load.

$$E_u = \frac{WV_{CMOD}(\alpha_c)}{C_u} \tag{4}$$

In order to find the critical crack length ratio, α_c, equations (1) and (4) are set equal, assuming the compliance change is only related to the crack extension. The critical crack length (a_c) can then be determined based on the specimen geometry, loading and unloading compliances, and initial notch length. The critical stress intensity factor, K_{IC}, at the peak load is then calculated using the geometric factor in Tada et al. (2000), $F(\alpha_c)$, and the applied nominal stress, σ:

$$K_{IC} = \sigma\sqrt{W}F(\alpha_c) \tag{5}$$

$$F(\alpha_c) = \frac{(2+\alpha_c)(0.76 + 4.8\alpha_c - 11.58\alpha_c^2 + 11.43\alpha_c^3 - 4.08\alpha_c^4)}{(1-\alpha_c)^{3/2}} \tag{6}$$

$$\sigma = \frac{P}{WB} \tag{7}$$

Since a crack opening displacement geometric factor for the initial crack tip is not available in the literature, a finite element analysis of the geometry was performed to obtain this geometric factor. The finite element model consisted of eight node quadrilateral (Q8) elements with a radial mesh at the notch tip. Figures 5a and 5b show the global mesh and the biased radial mesh towards the crack tip, respectively. The elements at the crack tip are collapsed Q8 elements with an average length of 0.03 mm and nodes at the quarter points. The quarter point elements enable the model to accurately represent the singular stress field at the crack front. The newly derived equation for $V_{CTOD}(\alpha_c)$, the CTOD geometric correction factor, is given in eq. 9.

$$CTOD_c = \frac{\sigma W V_{CTOD}(\alpha_c)}{E} \tag{8}$$

$$V_{CTOD}(\alpha_c) = 0.009621 \cdot \exp(35.35\alpha_c - 58.99\alpha_c^2 + 36.54\alpha_c^3) - 11.45 \tag{9}$$

The initial fracture properties are calculated from these equations and are provided in Table 3. The mean K_{IC} is greater for the LCA concrete (st. dev. = 0.119 MPa/m$^{1/2}$) relative to the RCA (st. dev. = 0.110 MPa/m$^{1/2}$) with the $CTOD_C$ values being similar. The total fracture energy, G_F, of the two concrete materials was calculated by dividing the area under the load-CMOD curve by the ligament area. The RCA concrete (st. dev. = 9.3 N/m) had slightly lower G_F relative to the LCA concrete (st. dev. = 15.3 N/m), which has been reported previously in SEN(B) tests (Bordelon et al. 2009). The coefficient of variation of all the fracture quantities were well within expected ranges (Bažant and Becq-Giraudon 2002c) and thus the preliminary experimental results suggest the DCT is a viable geometry for determining field fracture parameters. One specimen anomaly that caused some concern was the crack deviation angles. These ranged from 9° to 20° for the limestone specimens and 5° to 30° for the RCA specimens. The likely reason for this was

that the nominal maximum aggregate size was 25 mm, which is about 50 percent of the fracture length. Nevertheless, the deviations did not significantly affect the peak loads or fracture parameters.

Computational Crack Growth Modeling

A nonlinear finite element model was created to simulate the crack growth in the DCT specimens. Previous work had suggested that a cohesive zone model (Borst et al. 2004) with bilinear softening could adequately describe the fracture behavior of plain concrete (Petersson 1981, Gustafsson and Hillerborg 1985, Wittmann et al. 1988, Guinea et al. 1994, and Bažant 2002b, Roesler et al. 2007, Park et al. 2008).

Table 3. Experimental test results for all DCT specimens.

Specimen	P_c [kN]	G_F [N/m]	K_{IC} [MPa*m$^{1/2}$]	$CTOD_c$ [mm]	Averages
LCA-1	1.389	87.4	0.916	0.006	
LCA-2	1.159	87.6	0.998	0.009	G_F
LCA-3	1.612	123.0	1.161	0.009	100.1 N/m
LCA-4	1.421	98.7	1.117	0.009	K_{IC}
LCA-5	1.244	89.4	0.945	0.008	1.090 MPa*m$^{1/2}$
LCA-6	1.473	100.0	1.207	0.010	$CTOD_c$
LCA-7	1.262	94.4	1.179	0.011	0.009 mm
LCA-8	1.577	121.0	1.201	0.010	
RCA-1	1.029	111.0	1.011	0.012	
RCA-2	0.905	81.7	0.687	0.006	G_F
RCA-3	1.029	103.0	0.820	0.008	92.9 N/m
RCA-4	1.043	86.1	0.816	0.008	K_{IC}
RCA-5	1.008	87.9	0.807	0.008	0.816 MPa*m$^{1/2}$
RCA-6	0.959	96.0	0.722	0.006	$CTOD_c$
RCA-7	1.064	92.0	0.750	0.006	0.008 mm
RCA-8	1.102	85.4	0.918	0.009	

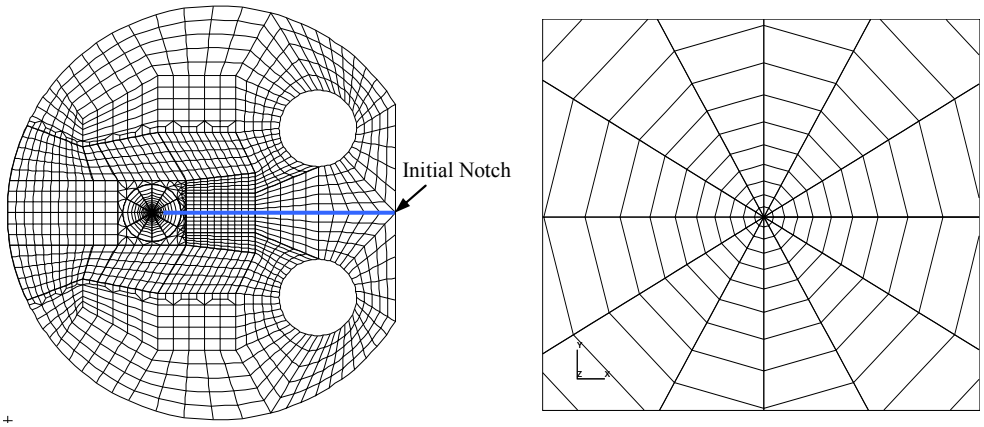

Figure 5. Example DCT finite element mesh: (a) global mesh, (b) biased radial mesh towards crack tip.

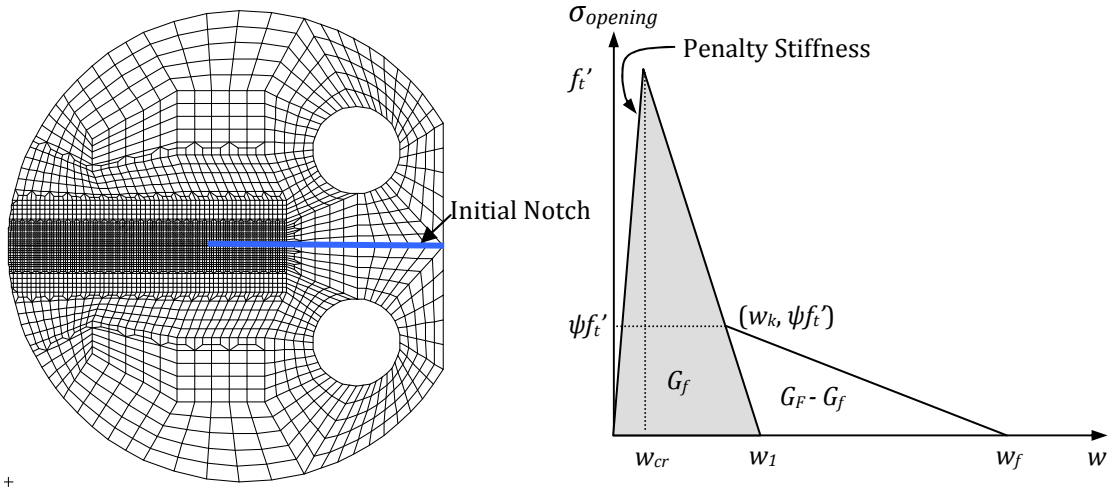

Figure 6. (a) DCT specimen with bulk and cohesive zone finite element mesh. (b) Cohesive stress-opening model with bilinear softening (Park et al., 2008).

Cohesive Zone Model

Figure 6a shows the finite element mesh used to simulate the mode I fracture of the DCT specimen. Linear elastic elements (Q4) were used in the model except in front of the crack tip. The cohesive zone model is implemented in commercial software (e.g. ABAQUS) as a user-defined subroutine. Cohesive elements were inserted in front of the initial crack tip and along the expected fracture path of the specimen. In order to model the fracture process accurately, the size of the cohesive crack elements was set to 0.7 mm, which is small enough to capture the nonlinear cohesive zone behavior. The bilinear softening model, shown in Figure 6b, was utilized to idealize the traction-separation relationship in front of the macro-crack tip.

Table 4. Bilinear cohesive model input parameters for limestone and RCA concrete.

Specimen	f_t [MPa]	G_f [N/m]	G_F [N/m]	CTODc [mm]	Ψ [%]
Limestone	3.3	26.50	100.1	0.0091	44.3
RCA	2.5	17.55	92.9	0.0079	45.0

The bilinear model inputs are the cohesive strength (e.g. tensile strength), f_t; the initial and total fracture energies, G_f and G_F respectively; the ratio of the kink point, ψ; and a parameter defining penalty stiffness, p. The experimentally determined input parameters for each material type are seen in Table 4. The tensile strength for the RCA concrete was lowered based on the additional split tensile strength tests, compressive strength results, and ultrasonic pulse velocity tests suggesting the RCA strength was approximately 25 percent lower than the LCA concrete. The initial fracture energy, G_f, was calculated from eq. 10.

$$G_f = \frac{K_{IC}^2}{E} \tag{10}$$

The kink point was defined (Park et al. 2008) at $(w_k, \psi f_t')$ where:

$$w_k = CTOD_c \tag{11}$$

$$\psi = 1 - \frac{CTOD_c f_t'}{2G_f} \tag{12}$$

The penalty stiffness was determined from the ratio of the opening displacement at the peak load, w_{cr}, to the final opening displacement, w_f, which was chosen to be equal to 0.01.

Simulation Results

The results of the finite element (FE) simulations are presented in Figures 3 and 4 for the LCA and RCA concrete. The cohesive zone model produced load versus CMOD curves that fell within the envelope of the experimental curves. There was a minor discrepancy observed between the experimental results and the computational model for the CMOD at the peak load. The experiments on the LCA specimens showed an average peak load of 1.39kN occurring at a CMOD of 0.067mm, while the FE model showed a peak load of 1.32kN occurring at a CMOD of 0.045mm. The experiments on the RCA specimens showed an average peak load of 1.02kN occurring at a CMOD of 0.072mm, while the FE model showed a peak load of 1.00kN occurring at a CMOD of 0.039mm.

Conclusions

Characterizing the mode I fracture properties of in-situ concrete is difficult with most of the current fracture specimen configurations used in the laboratory. Fracture properties are essential to accurately predict cracking behavior and load capacity of any concrete structure including concrete pavements. DCT specimens, 144 mm diameter by 51 mm, were extracted from several 15 cm thick slabs in order to test its viability to represent the fracture properties of recycled concrete aggregate (RCA) and limestone coarse aggregate concrete. A DCT geometry provided in the literature was utilized initially to calculate the fracture properties including the stress intensity factor and the critical crack length. A geometric correction factor for the CTOD was derived based on the finite element analysis of the DCT geometry with several initial crack lengths. The extracted fracture properties were similar to values presented in the literature for recycled and virgin concrete. The initial and total fracture energies were lower for the RCA concrete as expected. The tensile strength for RCA was estimated from the splitting test and ultrasonic pulse velocity measurements. A finite element-based cohesive crack model defined by the measured fracture properties (G_F, G_f, $CTOD_C$, f_t') was developed to simulate the load-CMOD curve of the two concrete materials. The numerical simulations reasonably matched the experimental data and correctly predicted the lower peak loads for the RCA concrete specimens. The results of this testing and modeling suggest that a DCT-type specimen can potentially provide useful mode I fracture properties of concrete.

Acknowledgements

We acknowledge the support from the National Science Foundation (NSF) through Grant CMMI #0800805. The information presented in this paper is the sole opinion of the authors and does not necessarily reflect the views of the sponsoring agency.

References

ASTM D7313-07b, 2007. Standard method for determining fracture energy of asphalt-aggregate mixtures using the disk-shaped compact tension geometry, ASTM International.

Bažant, Z. P., Qiang, Y., and Goanseup, Z. (2002a). "Choice of standard fracture test for concrete and its statistical evaluation." *Intl. J. Fracture*, 118, 303-337.

Bažant, Z. P. (2002b). "Concrete fracture models: Testing and practice," *Eng. Fracture Mech.*, 69, 165-205.

Bažant, Z. P., and Becq-Giraudon, E. (2002c). "Statistical prediction of fracture parameters of concrete and implications for choice of testing standard." *Cem. Con. Res.* 32 (4), 529-556.

Beckett, D. and Humphreys, J. (1989). *Comparative Tests on Plain, Fabric Reinforced and Steel Fibre Reinforced Concrete Ground Slabs,* Report No. TP/B/1, Thames Polytechnic School of Civil Engineering, Dartford, 33 pp.

Bordelon, A., Cervantes, V., Roesler, J. (2009). "Fracture properties of concrete containing recycled concrete aggregates." *Magazine of Concrete Research*, 61(9), 665-670.

Borst, R. de, Gutierrez, M.A., Wells, G.N., Remmers, J.J.C., Askes, H. (2004). "Cohesive zone models, higher-order continuum theories and reliability methods for computational failure analysis." *Int. J. for Numerical Methods in Eng.*, 60(1), 289–315.

Brühwiler, E., and Wittmann, F. H. (1990). "The wedge splitting test, a new method of performing stable fracture mechanics tests." *Eng. Fracture Mech.*, 35(1/2/3), 117-125.

Cusatis G., and Schauffert E. A., (2009). "Cohesive crack analysis of size effect." *Eng. Fracture Mech.*, 76, 2163-2173.

Darter, M. I. (1977). *Design of Zero-Maintenance Plain Jointed Concrete Pavement, Volume 1: Development of Design Procedures*. Federal Highway Administration Report No. FHWA-RD-77-III, Washington, DC.

Falkner, H., and Teutsch, M. (1993). *Comparative Investigations of Plain and Steel Fibre Reinforced Industrial Ground Slabs,* Institut Fur für Baustoffe, Massivbau und Brandschutz, Technical University of Brunswick, Germany, No. 102.

Gaedicke, C., Roesler, J. R., Shah, S. P. (2009a). "Fatigue crack growth prediction in concrete slabs." *Intl. J. Fatigue*, 31, 1309-1317.

Gaedicke, C. (2009b). "*Fracture-Based Method to Determine the Flexural Load Capacity of Concrete Slabs,*" Ph.D. thesis, University of Illinois, Urbana, Illinois.

Guinea, G. V., Planas, J., and Elices, M. (1994). "A general bilinear fit for the softening curve of concrete." *Mater. Struct.*, 27(2), 99–105.

Gustafsson, A., and Hillerborg, P. J. (1985). *Improvements in concrete design achieved through application of fracture mechanics*. In: Shah SP, editor. Application of fracture mechanics to cementious composites. The Netherlands: Dordrecht. p. 639–80

Ioannides, A. M. (2005). "Stress Prediction for Cracking of Jointed Plain Concrete Pavements, 1925–2000: An Overview." *Transportation Research Record; Journal of the Transportation Research Board, No. 1919*, Transportation Research Board of the National Academies, Washington, DC, pp.47-53.

Ioannides, A. M., Peng, J. and Swindler, J. R. (2006). "ABAQUS Model for PCC Slab Cracking." *Int. J. Pavement Eng.,* 7(4), 311-321.

Issa, M. A., Islam, M. S., and Chudnovsky, A. (2000a). "Size effects in concrete fracture: Part I, experimental setup and observations." *Int. J. Fracture*, 102, 1-24.

Issa, M. A., Islam, M. S., and Chudnovsky, A. (2000b). "Size effect in concrete fracture – Part II: Analysis of test results." *Int. J. Fracture*, 102, 15-42.

Jenq, Y. S., and Shah, S. P. (1985). "Two-Parameter Fracture Model for Concrete." *J. Eng. Mech.*, 111(4), 1227-1241.

Kim, H., and Buttlar, W. G. (2009). "Finite element cohesive fracture modeling of airport pavements at low temperatures." *Cold Regions Science and Technology*, 57, 123-130.

Kim, M., Buttlar, W. G., Baek, J., and Al-Qadi, I. L. (2009). "Field and laboratory evaluation of fracture resistance of Illinois hot-mix asphalt overlay mixtures," *Transportation Research Record; Journal of the Transportation Research Board, No. 2127*, Transportation Research Board of the National Academies, Washington, DC, pp. 146-154.

Kumar, S., and Barai, S. V. (2009). "Determining double-K fracture parameters of concrete for compact tension and wedge splitting tests using weight function." *Eng. Fracture Mech.*, 76, 935-948.

Park, K., Paulino, G. H., and Roesler, J. R. (2008). "Determination of the kink point in the bilinear softening model for concrete." *Eng. Fracture Mech.*, 75, 3806-3818.

Petersson, P. E. (1981). *Crack growth and development of fracture zone in plain concrete and similar materials.* Report No. TVBM-1006, Division of building materials, Lund Institute of Technology, Lund, Sweden.

Planas, J., Guinea, G. V., and Elices, M., 1999, "Size Effect and Inverse Analysis in Concrete Fracture." *Intl. J. Fracture*, 95, 367-378.

Rao, S., and Roesler, J. R. (2004). "Cumulative Fatigue Damage Analysis of Concrete Pavement using Accelerated Pavement Testing Results." Second International Conference on Accelerated Pavement Testing, September 25-29, 2004, Minneapolis, Minnesota.

RILEM, 1990, "Determination of Fracture Parameters (K_{IC} and $CTOD_C$) of Plain Concrete using Three-Point Bend Tests," RILEM Committee on Fracture Mechanics of Concrete-Test Methods, *Mat. Struct.*, 23, 457-460.

Roesler, J. R. (1998), *"Fatigue of Concrete Beams and Slabs*," Ph.D. thesis, University of Illinois, Urbana, IL.

Roesler, J. R., Hiller, J. E., and Littleton, P. C. (2005), "Large-Scale Airfield Concrete Slab Fatigue Tests," 8th International Conference on Concrete Pavement, August 13-18, 2005, Colorado Springs, CO, 23 pp.

Roesler, J. R., Paulino, G. H., Park, K. and Gaedicke, C. (2007). "Concrete fracture prediction using bilinear softening." *Cem. Con. Comp.*, 29, 300–312.

Song, S. H., Paulino, G. H., and Buttlar, W. B (2006). "Simulation of Crack Propagation in Asphalt Concrete Using a Cohesive Zone Model." *J. Eng. Mech.*, 123(11), 1215-1223.

Tada, H., Paris, P. C., and Irwin, G. R. (2000). The stress analysis of cracks handbook /New York: ASME Press

Van Mier, J. G. M. (1991). "Mode I Fracture Of Concrete: Discontinuous Crack Growth And Crack Interface Grain Bridging." *Cem. Conc. Res.*, 21(1), 1-15.

Wagoner, M. P., Buttlar, W. G., and Paulino, G. H. (2005). "Disk-shaped compact tension test for asphalt specimens." *Exp. Mech.*, 45(3), 270-277.

Wagoner, M. P., Buttlar, W. G. , Paulino, G. H., and Blankenship, P. I. (2006). "Laboratory Testing Suite for Characterization of Asphalt Concrete Mixtures Obtained from Field Cores." *J. Assoc. Asphalt Paving Technologists*, 75, 815-852.

Wittmann, F. H., Rokugo, K., Brühwiler, E., Mihashi, H., Simopnin, P. (1988). "Fracture energy and strain softening of concrete as determined by compact tension specimens." *Mater. Struct,*, 21(1), 21–32.

Zofka, A., and Braham, A. (2009). "Comparison of low-temperature field performance and laboratory testing of 10 test sections in the Midwestern United States," *Transportation Research Record; Journal of the Transportation Research Board, No. 2127*, Transportation Research Board of the National Academies, Washington, DC, pp. 107-114.